Contribution from the Department of Chemistry,
University of Victoria, Victoria, BC, V8W 2Y2 Canada

Synthesis of the Hexaamine Ligand 1,4,7-Tris(3-aminopropyl)-1,4,7-triazacyclononane: Reactivity and X-ray Crystal Structures of the Nickel(II) and Cobalt(III) Complexes
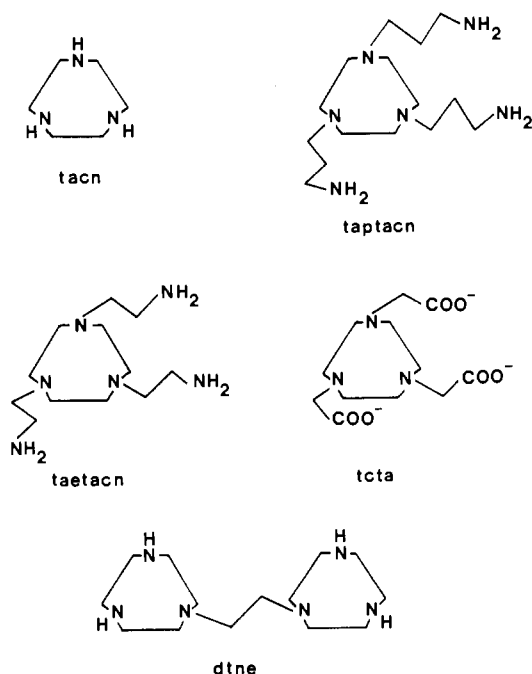
G. W. Bushnell,* D. G. Fortier, and A. McAuley*

The synthesis of the ligand 1,4,7-tris(3-aminopropyl)-1,4,7-triazacyclononane (taptacn) may be achieved by the reaction of 1,4,7-triazacyclononane with an excess of acrylonitrile, followed by reduction of the nitrile with sodium metal in toluene. Halide salts of the cobalt(III) (complex A) and nickel(II) (complex B) ions have been prepared and examined by using X-ray crystallography. Compound A, [Co(taptacn)]Br$_3$, crystallizes in the cubic space group $P2_13$, with $a = 12.871$ (2) Å, the asymmetric unit being one-third of a molecule, and four molecules per cell. The refinement converged at $R = 0.0257$ and $R_w = 0.0289$ with 619 observed reflections. The Co–N bond lengths were 2.025 (7) Å (tertiary amine) and 1.991 (6) Å (primary amine). The molecule has 3-fold symmetry and is chiral. The crystals of [Ni(taptacn)]Br$_2$·H$_2$O were triclinic, space group $P\bar{1}$, with two molecules in the asymmetric unit and four per cell: $a = 15.861$ (4) Å, $b = 16.388$ (5) Å, $c = 9.054$ (2) Å, $\alpha = 82.46$ (2)°, $\beta = 89.75$ (2)°, and $\gamma = 108.61$ (2)°. The refinement converged at $R = 0.0895$ and $R_w = 0.123$ for 451 parameters (50 anisotropic atoms, no H atoms), with use of 3935 reflections of intensities $I > 2\sigma(I)$. Ni–N(mean) = 2.141 Å. The Ni cation has approximately 3-fold symmetry. In reactions of the nickel(II) ion in aqueous acidic media, ready dissociation of the coordinated primary amines is observed with successive pK_a values of 4.18 ± 0.05, 4.91 ± 0.01, and 5.64 ± 0.02 for the tri-, di- and monoprotonated species. Oxidation of the Ni(taptacn)$^{2+}$ ion in CH$_3$NO$_2$ or CH$_3$CN with NO$^+$ gives rise to a Ni(III) species with axial symmetry ($g_\parallel = 2.033$, $g_\perp = 2.144$) characteristic of a low-spin d^7 system. Cyclic voltammetry in CH$_3$CN gives a reversible redox wave ($E_{1/2}$(Ni(taptacn)$^{3+/2+}$) = 1.172 V vs SCE). The ^{13}C NMR spectrum of the diamagnetic d^6 Co(III) complex ion shows five peaks, identifying a single isomer. At pH 7 (LiNO$_3$), there is a reversible cyclic voltammogram shown ($E_{1/2}$(Co(taptacn)$^{3+/2+}$) = -0.010 V). Optical activity of the cobalt(III) complex is observed, which has been used to derive the self-exchange rate constant for the Co(taptacn)$^{3+/2+}$ complex ($k_{exc} = 0.04$ M^{-1} s^{-1}). A comparative discussion of the two structures deals with ligand opening and with trigonal twist angle as related to metal ion size and mechanism for redox processes of the complexes.

There has been considerable recent interest in complexes containing macrocyclic ligands,[1,2] especially with regard to the stabilization of uncommon oxidation states of Ni,[3–5] Cu,[6] and Ru.[7] However, macrocycles, being not very flexible, may impose specific coordination geometries on the metal ion. Recently,[8–10] approaches have been taken to incorporate into the strongly binding segment of the macrocyclic framework more flexible pendant arms, with additional coordination sites, thus permitting the formation of stable metal complexes or groups for further reaction via functionalization. As an example of the former, Moore[11] has prepared quinquedentate pendant arm macrocyclic ligands that exhibit pH-dependent trigonal-bipyramidal–square-planar equilibria in the Ni(II) and Cu(II) species. Also, Hancock[10] has shown secondary binding of simple anions (Cl$^-$, Br$^-$, OH$^-$) to be important in the dicopper(II) complex of *N*,*N′*,*N″*,*N‴*-tetrakis(2-aminoethyl)cyclam.

Several complexes based on derivatives of 1,4,7-triazacyclononane (tacn) have been described. The hexadentate ligand 1,4,7-triazacyclononane-1,4,7-triacetate (tcta) binds M^{II} and M^{III} ions[12,13] (M = Cr, Mn, Fe, Co, Ni). Of interest is the nickel(II) complex, which may be isolated from nitric acid as a stabilized hydronium salt.[13] Other structural studies[12] show there is strain in the metal to ligand bonds with twisting of the acetate oxygen

tacn

taptacn

taetacn

tcta

dtne

donor atoms around the C_3 axis by up to 35° relative to the positions expected for regular octahedral coordination. Similar behavior has been observed in metal complexes of triaza macrocycles with three pendant arms.[14,15] The degree of twist correlates with the steric bulk of the attached units and is large in the Fe(II) complex containing pyridylmethyl arms. In this paper, we describe the synthesis of the hexacoordinate amine ligand 1,4,7-tris(3-aminopropyl)-1,4,7-triazacyclononane (taptacn). Crystal structures are consistent with coordination number 6. As with other ligands, it is anticipated that only slight changes take place in the primary coordination sphere on oxidation/reduction of the metal center in outer-sphere electron-transfer processes.

(1) Melson, G. A., Ed. *Coordination Chemistry of Macrocyclic Compounds*; Plenum: New York, 1979.
(2) Busch, D. H. *Adv. Chem. Ser.* **1971**, *No. 100*, 44; *Acc. Chem. Res.* **1978**, *11*, 392.
(3) Haines, R. I.; McAuley, A. *Coord. Chem. Rev.* **1981**, *39*, 77.
(4) Wieghardt, K.; Schmidt, W.; Herrmann, W.; Kuppers, H.-J. *Inorg. Chem.* **1983**, *22*, 2953.
(5) McAuley, A.; Norman, P. R.; Olubuyide, O. *Inorg. Chem.* **1984**, *23*, 1938.
(6) Fabbrizzi, L.; Poggi, A.; Zanello, P. *J. Chem. Soc., Dalton Trans.* **1984**, 1495. Fabbrizzi, L.; Kaden, T. A.; Perotti, A.; Seghi, B.; Siegfried, L. *Inorg. Chem.* **1986**, *25*, 321.
(7) Che, C. M.; Wong, K. Y.; Poon, C. K. *Inorg. Chem.* **1986**, *25*, 1809.
(8) Kaden, T. A. *Top. Curr. Chem.* **1984**, *121*, 157.
(9) Stetter, H. J.; Frank, W. *Angew. Chem.* **1976**, *88*, 760.
(10) Evers, A.; Hancock, R. D.; Murase, I. *Inorg. Chem.* **1986**, *25*, 2160.
(11) Alcock, N. W.; Kingston, R. G.; Moore, P.; Pierpoint, C. *J. Chem. Soc., Dalton Trans.* **1984**, 1937.
(12) Wieghardt, K.; Bossek, U.; Chaudhuri, P.; Herrmann, W.; Menke, B. C.; Weiss, J. *Inorg. Chem.* **1982**, *21*, 4308.
(13) vander Merve, M. J.; Boeyens, J. C. A.; Hancock, R. D. *Inorg. Chem.* **1985**, *24*, 1208.
(14) Chistiansen, L.; Hendrickson, D. N.; Toftlund, H.; Wilson, S. R.; Xie, C. L. *Inorg. Chem.* **1986**, *25*, 2813.
(15) Wieghardt, K.; Bossek, U.; Chaudhuri, P.; Herrmann, W.; Menke, B. C.; Weiss, J. *Inorg. Chem.* **1982**, *21*, 4308.

Characterization of the complexes is reported.

Experimental Section

All materials were of reagent grade, except where otherwise indicated. Infrared spectra were obtained as KBr disks or as neat samples on NaCl plates with a Perkin-Elmer 283 grating spectrometer. ^1H NMR spectra were measured on a 60-MHz Perkin-Elmer R12B spectrometer. High-field ^1H and ^{13}C NMR spectra were obtained with a Bruker WM 250 instrument. All chemical shifts are reported relative to tetramethylsilane (TMS).

ESR spectra were obtained at 77 K with a Varian E6S spectrometer and dpph (diphenylpicrylhydrazyl, $g = 2.0037$) as a reference standard.

UV–visible spectra were run on a Unicam SP800, a Cary 17, or a Perkin-Elmer Lambda 4B dual-beam spectrophotometer.

Elemental analyses were performed by Canadian Microanalytical Services, Vancouver, BC, Canada.

Kinetic Studies. $Co^{II}(L)$ solutions ($L = (tacn)_2$, sep, or taptacn) were prepared by reduction of their respective Co(III) complexes with zinc amalgam. $Co^{III}(tacn)_2^{3+}$ [16] and $Co^{III}(sep)^{3+}$ [17] (sep = sepulchrate = 1,3,6,8,10,13,16,19-octaazabicyclo[6.6.6]eicosane) were prepared by the literature methods.

Polarimetry kinetic studies were made on a Perkin-Elmer 141 polarimeter using the Na D line ($\lambda = 589$ nm) in 0.1 M LiNO$_3$. In order to prevent decomposition of the $Co^{II}(taptacn)$ complex, the pH was maintained at 9 with 0.01 M sodium borate.

Stopped-flow kinetic studies were carried out at $I = 0.1$ M (LiNO$_3$) by using an instrument described previously.[18] Linearity was observed over 2–3 half-lives. However, optical density changes were exceedingly small (<0.01 absorbance unit), which may have contributed to a greater degree of imprecision than usual for data of this type.

Electrochemistry. Electrochemical measurements were made by using a Princeton Applied Research Model 273 potentiostat/galvanostat. Under both aqueous and nonaqueous (CH$_3$CN) conditions, 0.1 M background electrolyte (LiNO$_3$ and n-Bu$_4$NClO$_4$, respectively) was always present. The working electrode was glassy carbon with Pt as the counter electrode. The reference electrode was a saturated calomel electrode linked to the cell via a bridge containing a saturated aqueous solution of KCl or a CH$_3$CN solution saturated with n-Bu$_4$NClO$_4$ for nonaqueous measurements. The complexes studied undergo rapid 1e redox reactions. In the cyclic voltammograms, the ratio of anodic to cathodic peaks was unity with typical S-shaped curves having $E_{3/4} - E_{1/4}$ = 60 mV.
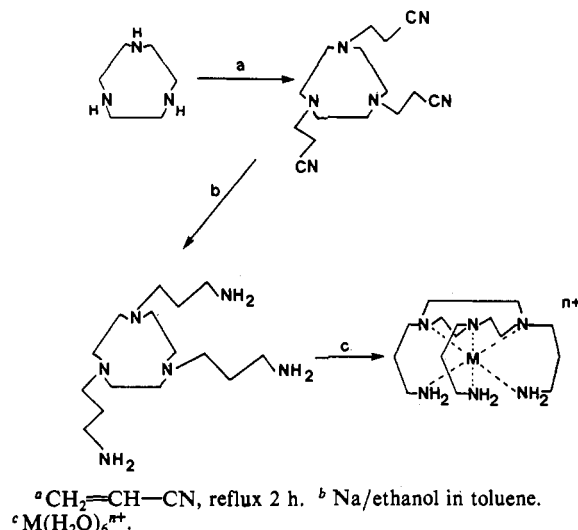
Determination of pK_a's. Titrations were carried out with a Metrohm 655 Dosimat microtitrator attached to a Metrohm 632 pH meter. The pH electrode (Fisher glass electrode) and the reference electrode (Fisher calomel electrode linked to the cell via a porous-plug bridge containing 0.1 M LiNO$_3$) were calibrated with commercially available buffers at pH 2.0 and 6.86, and linearity was checked at pH 4.1. The titrations were performed in a sealed cell under a slight positive pressure of argon. For pK_a determinations, a 5.5-mL solution of the complex ((1–2) × 10^{-3} M) containing excess base (NaOH, 2 mM) in 0.1 M LiCl or 0.1 M LiNO$_3$ was titrated by using standardized HNO$_3$ or HCl (~0.1 M) to beyond the end point (~400 μL) in 5-μL aliquots (18–22 points per proton equivalent). Back-titrations from excess acid with NaOH (0.1 M) yielded identical results. The data were processed by using SCOGS.[19] The final standard deviation in titer was less than 1 μL.

Preparation of the Ligand and Metal Complexes. The starting macrocycle (tacn) was prepared as described previously,[5] on the basis of a modification of the Richman–Atkins[20] synthesis. Reactions outlined in Scheme I led to the pure ligand.

1,4,7-Tris(2-cyanoethyl)-1,4,7-triazacyclononane (tcetacn). 1,4,7-Triazacyclononane (3.3 g, 25.6 mmol) was refluxed in acrylonitrile (50 mL) for 2 h under an atmosphere of nitrogen. The excess solvent was removed by evaporation in vacuo, leaving a creamy yellow solid (5.2 g, 70% yield). The product can be recrystallized from acetonitrile/diethyl ether (1:1), yielding a white crystalline solid, mp 160 °C. ^1H NMR (CD$_3$CN, δ): 2.80 (t, 6, CH$_2$CN, $J = 7.0$ Hz); 3.07 (s, 12, NCH$_2$CH$_2$N); 3.15 (t, 6, NCH_2CH$_2$CN, $J = 7.0$ Hz). ^{13}C NMR (CD$_3$CN, δ): 16.75 (CH$_2$CN); 53.11 (NCH$_2$CH$_2$N); 53.36 (NCH$_2$-CH$_2$CN); 120.48 (CN). Mass spectrum (m/e): 289 (M + 1); 248 (M – CH$_2$CN). IR (cm^{-1}): 2240 (CN).

1,4,7-Tris(3-aminopropyl)-1,4,7-triazacyclononane (taptacn). Sodium metal (5.8 g) was suspended in refluxing toluene (200 mL). To this

(16) Koyama, H.; Yoshino, T. *Bull. Chem. Soc. Jpn.* **1972**, *45*, 481.
(17) Creaser, I. I.; Geue, R. J.; Harrowfield, J. M.; Herlt, A. J.; Sargeson, A. M.; Snow, M. R.; Springborg, J. *J. Am. Chem. Soc.* **1982**, *104*, 6016.
(18) Ellis, K. J.; McAuley, A. *J. Chem. Soc., Dalton Trans.* **1973**, 1533.
(19) Sayce, I. *Talanta* **1968**, *15*, 1397; **1971**, *18*, 653.
(20) Atkins, T. J.; Richman, J. E.; Oettle, W. F. *Org. Synth.* **1978**, *58*, 86.

Scheme I. Synthetic Route to M(taptacn)$^{n+}$

^{a}CH$_2$=CH—CN, reflux 2 h. ^{b}Na/ethanol in toluene. ^{c}M(H$_2$O)$_6^{n+}$.

mixture was added dropwise a solution of tcetacn (4.0 g, 14 mmol) in absolute ethanol (25 mL) over a 2-h period. The mixture was further refluxed for another 90 min, at which point all the sodium had dissolved. After the mixture was cooled, the precipitate formed was removed by filtration and rinsed with toluene several times. The toluene fractions were evaporated under vacuum, and the residue was subsequently extracted with hot petroleum ether (10 × 50 mL). The combined fractions were filtered, and on removal of solvent, a pale yellow oil remained (2.5 g, 65% yield; this oil was used without further purification in the preparation of metal complexes). ^1H NMR (CD$_3$CN, δ): 1.32 (s, 6, NH$_2$); 1.45 (q, 6, CH$_2$CH_2CH$_2$NH$_2$, $J = 6.9$ Hz); 2.45 (t, 6, CH_2NH$_2$, $J = 6.9$ Hz); 2.60 (t, 6, NCH_2CH$_2$CH$_2$, $J = 6.9$ Hz); 2.65 (s, 12, NCH_2CH_2N). ^{13}C NMR (CDCl$_3$, δ): 28.19 (CH$_2$CH$_2$CH$_2$); 39.16 (CH$_2$NH$_2$); 51.87 (NCH$_2$CH$_2$N); 55.17 (NCH$_2$CH$_2$CH$_2$). IR (cm^{-1}): 3300, 3370 (NH).

[Ni(taptacn)](ClO$_4$)$_2$. To taptacn (1.4 g, 4.7 mmol) dissolved in hot ethanol (300 mL) was added a solution (50 mL, 80% ethanol/water) containing nickel(II) acetate (1.16 g, 4.7 mmol). The purple coloration appeared immediately, but stirring was continued for another 30 min. After the mixture was cooled, the volume was reduced to 40 mL (evaporation under vacuum). To this solution was added saturated aqueous sodium perchlorate (5 mL) to precipitate the purple perchlorate salt. The material was filtered, washed with cold ethanol, and air-dried (1.2 g, 46% yield). Anal. Calcd for [Ni(C$_{15}$H$_{36}$N$_6$)](ClO$_4$)$_2$: C, 32.28; H, 6.50; N, 15.05; Cl, 12.70; O, 22.93. Found: C, 32.24; H, 6.51; N, 14.80; Cl, 12.75; O, 22.78.

[Ni(taptacn)]Br$_2$·H$_2$O (Compound B). The nickel(II) taptacn complex was prepared as above. Addition of saturated aqueous NaBr (5 mL) yielded purple crystals overnight (1.0 g, yield 40%). Anal. Calcd for [Ni(C$_{15}$H$_{36}$N$_6$)]Br$_2$·H$_2$O: C, 33.54; H, 7.13; N, 15.64; Br, 29.75. Found: C, 32.73; H, 7.03; N, 14.89; Br, 28.44.

[Co^{III}(taptacn)]Cl$_3$·H$_2$O. To a solution of taptacn (4 g, 13.3 mmol) in water (100 mL) was added an aqueous solution (50 mL) containing CoCl$_2$·6H$_2$O (3.2 g, 13.4 mmol). Activated charcoal (1 g) and HCl (3.5 mL of 4 M stock) were also added. Air was bubbled through the mixture for 4 h. After filtration, the dark orange-red solution was transferred to a column of Dowex 50X8-400 ion-exchange resin in the H$^+$ form (4.5 × 15 cm column); washing with 1.5 M HCl removed residual cobalt(II). The complex was eluted as a pink band with 4 M HCl. On evaporation to dryness, the residue was treated with an 80% ethanol/water solution, whereupon an orange powder formed. This was filtered, washed with cold ethanol, and air-dried (yield 3.88 g). The material was recrystallized from hot water/DMSO, producing yellow-brown crystals. ^{13}C NMR (D$_2$O, δ): 23.50 (CH$_2$CH$_2$CH$_2$); 37.95 (CH$_2$NH$_2$); 57.33, 62.08, 66.26 (CH$_2$N). Anal. Calcd for [Co(C$_{15}$H$_{36}$N$_6$)]Cl$_3$: C, 38.70; H, 7.70; N, 18.10; Cl, 22.80. Found: C, 38.43; H, 7.70; N, 17.61; Cl, 22.90.

[Co^{III}(taptacn)]Br$_3$ (Compound A). To a solution of Co^{III}(taptacn)Cl$_3$ in hot water was added a saturated solution of NaBr. The precipitate that formed upon cooling was further recrystallized (four times) from aqueous NaBr solutions, yielding X-ray-quality crystals. Anal. Calcd for [Co(C$_{15}$H$_{36}$N$_6$)]Br$_3$: C, 30.07; H, 6.05; N, 14.02; Br, 40.01. Found: C, 29.91; H, 6.09; N, 13.91; Br, 39.44.

X-ray Crystallography. Compound A. The orange crystal was small, well-formed and hexagonal; its dimensions were approximately 0.4 × 0.4 × 0.2 mm. Lack of extinction under the polarizing microscope suggested cubic symmetry. The specimen was mounted and centered on a Nonius

Table I. Experimental Crystallographic Data

Compound A

space group: $P2_13$
$a = 12.871$ (2) Å
V(cell) $= 2132$ (1) Å^3, $Z = 4$ molecules/cell, asymmetric unit $^1/_3$ molecule
D(calcd) $= 1.866$, D(measd) $= 1.849$ g cm^{-3}
diffractometer: Nonius CAD4, Mo Kα_1, graphite monochromator, $\lambda = 0.709\,30$ Å
measurements: $2\theta = 2-50°$, 1 octant
scan width: $0.80 + 0.34 \tan \theta$
no. of indep obsd rflns: 619 $(I > 2.5\sigma(I))$
$R = 0.0257$, $R_w = 0.0289$, GOF $= 3.239$
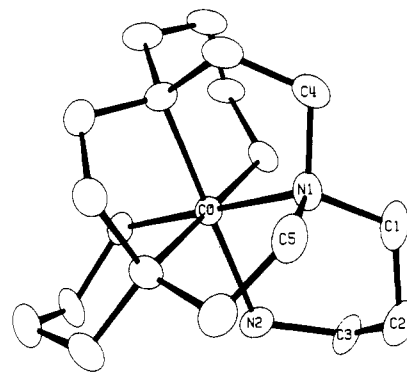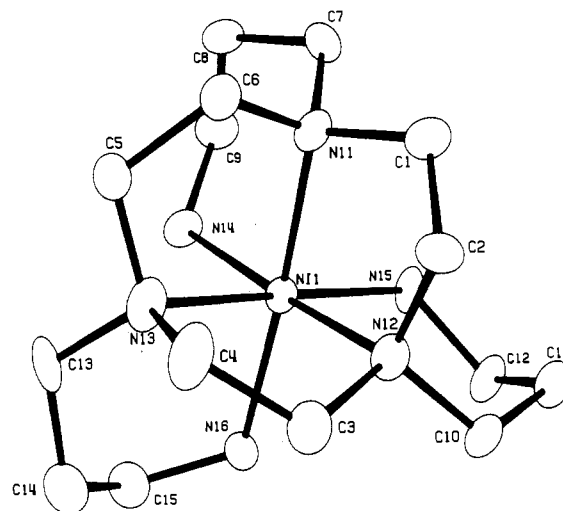abs cor (spherical): $\mu = 63.84$ cm^{-1}

Compound B

space group: $P\bar{1}$
$a = 15.861$ (4), $b = 16.388$ (5), $c = 9.054$ (2) Å
$\alpha = 82.46$ (2), $\beta = 89.75$ (2), $\gamma = 108.61$ (2)°
V(cell) $= 2208.4$ (9) Å^3, $Z = 4$ molecules/cell, asymmetric unit 2 molecules
D(calcd) $= 1.615$, D(measd) $= 1.609$ g cm^{-3}
diffractometer: Picker with PDP11/10, $\lambda = 0.710\,69$ Å
measurements: $2\theta = 2-45°$, 1 hemisphere
scan width: $1.2°$ in 2θ
no. of measurements: 3935 $(I > 2\sigma(I))$
$R = 0.895$, $R_w = 0.123$
abs cor: by numerical integration of $8 \times 8 \times 16$ Gaussian grid, $\mu = 44.82$ cm^{-1}
transmission factors: 0.265–0.756
cryst shape (indices, perpendicular dist to origin (mm)):
± 100, 0.1414; ± 010, 0.0296; ± 001, 0.2944

CAD4 diffractometer. Crystal data are given in Table I. The experimental work was carried out at 20 °C. Intensity measurements were made with Mo radiation filtered through a graphite monochromator, $\lambda = 0.709\,300$ Å. The cell was refined by using 21 centered reflections in the range $\theta = 15-23°$. A prescan and a variable-speed final scan were used. A set of three standards was measured hourly, and the orientation was checked every 500 reflections. The total number of reflections measured was 2294, but this reduced to 716 independent reflections, of which 619 were fully observed. The intensity measurements were corrected for Lorentz and polarization effects, and for absorption by using the approximation that the crystal was spherical (diameter 0.25 mm).

The crystal structure was solved and refined by the use of a program package written at the National Research Council of Canada.[21] The atomic scattering factors, together with the Co f curves, were taken from ref 22. The phase problem was solved by use of symmetry and the Patterson function. The completion of the structure was done with difference electron density maps. The refinement was by least squares minimizing $\sum w\Delta^2$, where $w = 1/\sigma^2(F)$ and $\Delta = ||F_o| - |F_c||$.

All non-hydrogen atoms were given anisotropic temperature parameters. The symmetry restraints on these parameters were applied by the program. An R value of 0.0354 was obtained before hydrogen atoms were introduced into the calculation. Minor difficulties were experienced with a few of the hydrogen atoms, and so for the sake of uniformity they were all placed at calculated positions (C–H and N–H = 1.08 Å). The final refinement converged to $R = 0.0257$ and $R_w = 0.0289$. The goodness of fit was 3.239. A final difference map was used to check for any further material in the structure. The maximum value was 35 on an arbitrary scale on which the standard deviation of the map values was 8.9. The supplementary material deposited contains the structure factors, the anisotropic temperature parameters, ligand bite and torsion angles, and information related to the hydrogen atom positions used.

Compound B. The magenta/purple crystals were subjected to Weissenberg and precession photography to establish the symmetry and cell dimensions. The crystal data are given in Table I. The formula is $C_{15}H_{38}Br_2N_6NiO$; $M_r = 537.01$. The crystal was mounted on a glass fiber directed along the c axis. The specimen showed clean extinction between crossed polarizers. The crystal dimensions were $0.283 \times 0.059 \times 0.589$ mm. The experimental work was done at a temperature of 20 °C. After photography, the crystal was transferred to a Picker four-circle diffractometer automated with a PDP11/10 computer. The unit cell was

(21) Le Page, Y.; Gabe, E. J.; White, P. S. "NRCCAD Modification of the Enraf-Nonius Program"; Chemistry Division, National Research Council of Canada: Ottawa, Canada.
(22) *International Tables for X-ray Crystallography*; Kynoch: Birmingham, U.K., 1974; Vol. IV.

Figure 1. Molecular structure of compound A showing 50% thermal ellipsoids.

Figure 2. Molecular structure of compound B showing 25% thermal ellipsoids.

refined by using 26 pairs of reflections in the 2θ range 14–41°. Intensity measurements were carried out with Zr-filtered Mo radiation, $\lambda = 0.710\,69$ Å.

The scanning was done in the $\theta/2\theta$ mode by using 120 steps of $0.01°$ in 2θ and counting for 0.25 s per step. Background counting was for 15 s at each end of the scan. A set of three standard reflections preceded each batch of 50 measurements. A total of 5185 independent reflections were measured.

The solution of the phase problem was by direct method with SHELX-76.[23] The atomic scattering factors used were those included in the SHELX-76 program together with the Ni f curve from ref 22. Completion and refinement of the structure was done by difference electron density maps and by least squares minimizing $\sum_w\Delta^2$, where $\Delta = ||F_o| - F_c||$ and $w = 1/(\sigma^2(F) + 0.001F^2)$. The asymmetric unit consisted of two coordination complexes, four bromide ions, and two water molecules of crystallization. Hydrogen atoms were not included in the calculations. All included atoms were treated by using anisotropic thermal vibration parameters. There were 50 atoms in the asymmetric unit and 451 parameters to be refined. The four Br atoms and the two O atoms were refined in each cycle, and the rest of the structure was refined in alternating cycles of least squares, each containing one whole metal complex. The refinement converged with a maximum shift/esd of 0.026 on the final cycle. $R = 0.0895$; $R_w = 0.123$. A final difference map had a maximum peak of 2.1 e Å^{-3} that was unconnected and that when included as an oxygen of a water molecule gave a site occupancy factor of 0.488 without a significant decrease in the R value; it was thus left out. Tables containing structure factors, anisotropic temperature parameters, and intermolecular distances have been deposited as supplementary material.

Results and Discussion

Excellent reproducibility in the ligand synthesis was observed, and under conditions of dry atmosphere a white hygroscopic solid

(23) Sheldrick, G. M. "SHELX76, Program for Crystal Structure Refinement"; University of Cambridge: Cambridge, U.K., 1976.

Table II. Fractional Atomic Coordinates and Isotropic Temperature Factors for Compound A

	x/a	y/b	z/c	U(iso), Å$^{2\,a}$
Br(1)	0.81447 (7)	0.81447	0.81447	0.0385 (3)
Br(2)	0.02335 (6)	0.02335	0.02335	0.0312 (3)
Br(3)	0.57328 (8)	0.57328	0.57328	0.0412 (3)
Co	0.21085 (8)	0.21085	0.21085	0.0197 (3)
N(1)	0.2476 (5)	0.3625 (5)	0.1898 (6)	0.025 (4)
N(2)	0.2326 (5)	0.1765 (5)	0.0614 (5)	0.024 (4)
C(1)	0.2181 (7)	0.4109 (7)	0.0864 (7)	0.038 (5)
C(2)	0.2551 (7)	0.3537 (7)	−0.0080 (7)	0.035 (5)
C(3)	0.2020 (7)	0.2507 (7)	−0.0228 (6)	0.033 (5)
C(4)	0.1902 (6)	0.4201 (6)	0.2732 (6)	0.029 (5)
C(5)	0.3655 (6)	0.3756 (7)	0.2047 (7)	0.034 (5)

$^a U$(iso) is the mean of the principal axes of the thermal ellipsoid.

Table III. Fractional Atomic Coordinates and Temperature Parameters for Compound B^a

atom	x/a	y/b	z/c	U(eq), Å^2
Br(1)	65529 (11)	42806 (11)	58778 (18)	463 (7)
Br(2)	37022 (12)	14968 (12)	7742 (21)	553 (8)
Br(3)	85582 (12)	16087 (13)	59180 (22)	604 (8)
Br(4)	14590 (11)	38754 (11)	−3761 (18)	437 (7)
O(1)	3501 (11)	−15 (10)	3886 (18)	98 (8)
O(2)	1590 (9)	147 (10)	1451 (16)	85 (7)
Ni(1)	20343 (13)	25223 (12)	62201 (21)	334 (8)
N(11)	3291 (8)	2865 (9)	5012 (14)	46 (6)
N(12)	1506 (9)	2331 (9)	4065 (14)	43 (6)
N(13)	2087 (10)	1218 (9)	6294 (16)	57 (7)
N(14)	2670 (8)	2715 (9)	8300 (14)	42 (5)
N(15)	1969 (9)	3810 (8)	5979 (14)	43 (6)
N(16)	770 (8) ·	2077 (9)	7469 (15)	46 (6)
C(1)	3124 (11)	3203 (12)	3495 (18)	47 (7)
C(2)	2254 (10)	2581 (11)	2922 (19)	47 (7)
C(3)	1073 (12)	1363 (11)	4164 (19)	52 (7)
C(4)	1682 (14)	873 (11)	4874 (21)	67 (9)
C(5)	3054 (11)	1338 (11)	6220 (19)	47 (8)
C(6)	3561 (11)	2078 (11)	5040 (18)	49 (7)
C(7)	4024 (10)	3593 (11)	5544 (19)	50 (7)
C(8)	4202 (10)	3380 (12)	7191 (19)	52 (8)
C(9)	3501 (12)	3471 (13)	8255 (21)	59 (8)
C(10)	836 (11)	2745 (11)	3590 (19)	46 (7)
C(11)	1117 (11)	3724 (11)	3653 (19)	50 (8)
C(12)	1161 (11)	3951 (11)	5262 (18)	48 (7)
C(13)	1680 (13)	599 (11)	7604 (20)	60 (8)
C(14)	688 (13)	517 (12)	8063 (25)	71 (9)
C(15)	580 (12)	1306 (12)	8653 (21)	59 (8)
Ni(2)	71373 (12)	29000 (12)	−902 (22)	347 (8)
N(21)	8397 (8)	3270 (8)	905 (14)	40 (5)
N(22)	6625 (8)	2695 (8)	2150 (14)	42 (5)
N(23)	7196 (9)	1608 (8)	521 (15)	44 (6)
N(24)	7748 (8)	3078 (8)	−2284 (12)	36 (5)
N(25)	7048 (8)	4173 (8)	−498 (13)	38 (5)
N(26)	5886 (8)	2448 (8)	−1053 (15)	45 (6)
C(21)	8224 (11)	3632 (12)	2293 (17)	51 (8)
C(22)	7413 (12)	3010 (13)	3137 (19)	57 (8)
C(23)	6177 (13)	1719 (12)	2563 (22)	65 (9)
C(24)	6800 (14)	1249 (12)	2034 (24)	72 (10)
C(25)	8151 (15)	1752 (12)	746 (21)	63 (9)
C(26)	8686 (13)	2488 (12)	1319 (21)	62 (9)
C(27)	9128 (11)	3983 (11)	7 (17)	47 (7)
C(28)	9329 (11)	3822 (11)	−1553 (20)	52 (7)
C(29)	8604 (10)	3852 (11)	−2685 (20)	49 (7)
C(30)	5912 (11)	3112 (11)	2441 (20)	61 (8)
C(31)	6169 (11)	4075 (11)	1904 (19)	47 (7)
C(32)	6236 (12)	4311 (12)	229 (17)	50 (8)
C(33)	6801 (14)	1002 (11)	−619 (26)	74 (10)
C(34)	5849 (13)	912 (13)	−895 (24)	70 (9)
C(35)	5716 (12)	1689 (12)	−1921 (21)	59 (8)

^{a} Estimated standard deviations are given in parentheses. Coordinates are $\times 10^n$, where $n = 5$ for Br and Ni and $n = 4$ otherwise. Temperature parameters are $\times 10^n$, where $n = 4$ for Br and Ni and $n = 3$ otherwise. U(eq) is the equivalent isotropic temperature parameter: $U(\text{eq}) = \frac{1}{3}\sum_i\sum_j U_{ij}a_i^* a_j^* (a_i \cdot a_j)$. $T = \exp[-8\pi^2(U(\text{iso}))(\sin^2 \theta)/\lambda^2]$.

was obtained. However, when the solid stood, especially in light, a pale yellow oil was obtained, which turned progressively darker.

Table IV. Bond Lengths and Angles for Compound A

(a) Bond Lengths (Å)			
Co(1)–N(1)	2.025 (7)	N(2)–C(3)	1.496 (10)
Co(1)–N(2)	1.991 (6)	C(1)–C(2)	1.498 (14)
N(1)–C(1)	1.517 (11)	C(2)–C(3)	1.502 (12)
N(1)–C(4)	1.498 (11)	C(4)–C(5)^b	1.505 (12)
N(1)–C(5)	1.537 (11)		

(b) Bond Angles (deg)			
N(1)–Co(1)–N(1)^a	86.3 (3)	C(1)–N(1)–C(4)	107.5 (6)
N(1)–Co(1)–N(2)	93.0 (3)	C(1)–N(1)–C(5)	108.1 (6)
N(1)–Co(1)–N(2)^a	179.2 (3)	C(4)–N(1)–C(5)	110.1 (6)
N(1)–Co(1)–N(2)^b	93.5 (3)	Co(1)–N(2)–C(3)	121.3 (5)
N(2)–Co(1)–N(2)^a	87.3 (3)	N(1)–C(1)–C(2)	115.4 (7)
Co(1)–N(1)–C(1)	117.0 (5)	C(1)–C(2)–C(3)	113.1 (7)
Co(1)–N(1)–C(4)	105.4 (5)	N(2)–C(3)–C(2)	110.6 (7)
Co(1)–N(1)–C(5)	108.6 (5)	N(1)–C(4)–C(5)^b	109.5 (6)
		N(1)–C(5)–C(4)	110.5 (7)

^{a} Symmetry position y, z, x. ^{b} Symmetry position z, x, y.

For this reason, preparation of the metal complexes was undertaken immediately after isolation of the ligand.

Reaction of equimolar quantities of the ligand with transition-metal ions in ethanol yielded the nickel(II) compound, while the cobalt(III) compound could be prepared in aqueous media.

Molecular Structures. The molecular structures of the complexes are shown in Figures 1 and 2. In a broad sense they are much the same. The cobalt complex is the simpler to describe because of its high symmetry, which includes a 3-fold axis within the molecule. In the space group, the Co atom is in a special position (Wyckoff type a) of multiplicity 4 and site symmetry 3. The nickel complex has two molecules in the asymmetric unit, and it follows that each of these is individually devoid of symmetry. We have not detected any major differences between the two independent Ni complexes. However, the differences between the Co and Ni complexes are both significant and interesting. The fractional atomic coordinates of the cobalt complex (A) are given in Table II. The heavy atoms are in special positions; thus, each provides only one positional variable. The molecule consists of a triply charged complex cation and three separate bromide anions. The atomic labeling scheme is displayed in Figure 1. The cation is shown, and only the atoms of the asymmetric unit are labeled. The asymmetric unit is repeated by a 3-fold symmetry axis to form the molecule. The fractional atomic coordinates for the Ni complex (B) are given in Table III for the two crystallographically independent formula units that comprise the asymmetric unit. Such behavior is unusual but not rare. The unit cell was checked for additional symmetry by using a program that searches for 2-fold axes,[24] but none were found. Each formula unit consists of a doubly charged Ni(II) cation, two bromide anions, and a water molecule. The isotropic temperature parameters given are calculated from the anisotropic parameters, which were used and have been deposited as supplementary material.

Table IV gives both the bond lengths and the bond angles for compound A. The difference between the two independent Co–N bond lengths is 0.033 (10) Å and is perceptible. The small difference suggests that the macrocyclic N atoms (tertiary) have the longer bonds to Co, in contrast to the situation observed in Co(taetacn)$^{3+}$ [25] (taetacn = 1,4,7-tris(2-aminoethyl)-1,4,7-triazacyclononane), where Co^{III}–N(primary) = 2.009 Å and Co^{III}–N(tertiary) = 1.963 Å. It is also of interest that in the structure the Co^{III}–N bonds are longer than the normal bond distance of 1.97 Å[4,26] This is also the average bond length found in the 2-methyl tacn derivative [Co((R)-Metacn)2]I$_3$·5H$_2$O,[27] in which the average N–Co–N bond angle within one coordinated triazacyclononane ring is 85°. In complex A, the bond angles at Co

(24) Le Page, Y. *J. Appl. Crystallogr.* **1982**, *15*, 255.
(25) Taylor, S. G.; Snow, M. R.; Hambley, T. W. *Aust. J. Chem.* **1983**, *36*, 2359.
(26) Thom, V. J.; Boeyens, J. C. A.; McDougall, G. J.; Hancock, R. D. *J. Am. Chem. Soc.* **1984**, *106*, 3198.
(27) Mikami, M.; Kuroda, R.; Konno, M.; Saito, Y. *Acta Crystallogr., Sect. B: Struct. Crystallogr. Cryst. Chem.* **1977**, *B33*, 1485.

Table V. Interatomic Distances for Compound B (Å)[a]

N(11)–Ni(1)	2.142 (13)	N(21)–Ni(2)	2.135 (13)
N(12)–Ni(1)	2.148 (13)	N(22)–Ni(2)	2.125 (13)
N(13)–Ni(1)	2.16 (2)	N(23)–Ni(2)	2.15 (2)
N(14)–Ni(1)	2.152 (13)	N(24)–Ni(2)	2.149 (12)
N(15)–Ni(1)	2.128 (14)	N(25)–Ni(2)	2.120 (14)
N(16)–Ni(1)	2.159 (13)	N(26)–Ni(2)	2.120 (12)
C(1)–N(11)	1.47 (2)	C(21)–N(21)	1.52 (2)
C(6)–N(11)	1.48 (3)	C(26)–N(21)	1.50 (3)
C(7)–N(11)	1.51 (2)	C(27)–N(21)	1.50 (2)
C(2)–N(12)	1.49 (2)	C(22)–N(22)	1.53 (2)
C(3)–N(12)	1.51 (2)	C(23)–N(22)	1.52 (2)
C(10)–N(12)	1.47 (2)	C(30)–N(22)	1.54 (3)
C(4)–N(13)	1.53 (3)	C(24)–N(23)	1.47 (2)
C(5)–N(13)	1.48 (2)	C(25)–N(23)	1.46 (3)
C(13)–N(13)	1.45 (2	C(33)–N(23)	1.52 (3)
C(9)–N(14)	1.49 (2)	C(29)–N(24)	1.54 (2)
C(12)–N(15)	1.51 (2)	C(32)–N(25)	1.54 (2)
C(15)–N(16)	1.49 (2)	C(35)–N(26)	1.51 (3)
C(2)–C(1)	1.57 (2)	C(22)–C(21)	1.49 (2)
C(4)–C(3)	1.53 (3)	C(24)–C(23)	1.54 (3)
C(6)–C(5)	1.51 (2)	C(26)–C(25)	1.53 (3)
C(8)–C(7)	1.54 (2)	C(28)–C(27)	1.52 (3)
C(9)–C(8)	1.52 (3)	C(29)–C(28)	1.55 (2)
C(11)–C(10)	1.53 (3)	C(31)–C(30)	1.51 (2)
C(12)–C(11)	1.55 (3)	C(32)–C(31)	1.51 (2)
C(14)–C(13)	1.59 (3)	C(34)–C(33)	1.50 (3)
C(15)–C(14)	1.52 (3)	C(35)–C(34)	1.55 (3)

[a] Estimated standard deviations are given in parentheses.

Table VI. Bond Angles for Compound B (deg)[a]

N(12)–Ni(1)–N(11)	83.4 (5)	N(22)–Ni(2)–N(21)	83.6 (5)
N(13)–Ni(1)–N(11)	83.2 (6)	N(23)–Ni(2)–N(21)	83.3 (5)
N(13)–Ni(1)–N(12)	84.4 (6)	N(23)–Ni(2)–N(22)	82.1 (5)
N(14)–Ni(1)–N(11)	91.8 (5)	N(24)–Ni(2)–N(21)	92.4 (5)
N(14)–Ni(1)–N(12)	175.1 (5)	N(24)–Ni(2)–N(22)	175.2 (5)
N(14)–Ni(1)–N(13	93.8 (6)	N(24)–Ni(2)–N(23)	95.0 (5)
N(15)–Ni(1)–N(11)	95.4 (5)	N(25)–Ni(2)–N(21)	95.6 (5)
N(15)–Ni(1)–N(12)	91.6 (5)	N(25)–Ni(2)–N(22)	93.0 (5)
N(15)–Ni(1)–N(13)	175.9 (5)	N(25)–Ni(2)–N(23)	175.0 (5)
N(15)–Ni(1)–N(14)	90.1 (5)	N(25)–Ni(2)–N(24)	89.8 (5)
N(16)–Ni(1)–N(11)	175.6 (6)	N(26)–Ni(2)–N(21)	176.3 (5)
N(16)–Ni(1)–N(12)	96.7 (5)	N(26)–Ni(2)–N(22)	96.2 (5)
N(16)–Ni(1)–N(13)	92.5 (6)	N(26)–Ni(2)–N(23)	92.9 (5)
N(16)–Ni(1)–N(14)	87.9 (5)	N(26)–Ni(2)–N(24)	87.8 (5)
N(16)–Ni(1)–N(15)	89.0 (5)	N(26)–Ni(2)–N(25)	88.1 (5)
C(1)–N(11)–Ni(1)	104.6 (10)	C(21)–N(21)–Ni(2)	104.3 (10)
C(6)–N(11)–Ni(1)	109.0 (9)	C(26)–N(21)–Ni(2)	109.9 (9)
C(6)–N(11)–C(1)	112.0 (14)	C(26)–N(21)–C(21)	110.5 (13)
C(7)–N(11)–Ni(1)	114.8 (11)	C(27)–N(21)–Ni(2)	115.8 (10)
C(7)–N(11)–C(1)	105.7 (12)	C(27)–N(21)–C(21)	106.1 (12)
C(7)–N(11)–C(6)	110.7 (13)	C(27)–N(21)–C(26)	110.1 (13)
C(2)–N(12)–Ni(1)	109.3 (9)	C(22)–N(22)–Ni(2)	107.9 (9)
C(3)–N(12)–Ni(1)	104.6 (9)	C(23)–N(22)–Ni(2)	106.8 (11)
C(3)–N(12)–C(2)	106.7 (14)	C(23)–N(22)–C(22)	109.8 (13)
C(10)–N(12)–Ni(1)	117.3 (11)	C(30)–N(22)–Ni(2)	116.2 (10)
C(10)–N(12)–C(2)	110.6 (12)	C(30)–N(22)–C(22)	110.3 (14)
C(10)–N(12)–C(3)	107.8 (12)	C(30)–N(22)–C(23)	105.8 (12)
C(4)–N(13)–Ni(1)	107.6 (12)	C(24)–N(23)–Ni(2)	110.6 (13)
C(5)–N(13)–Ni(1)	103.8 (10)	C(25)–N(23)–Ni(2)	102.3 (10)
C(5)–N(13)–C(4)	108.7 (15)	C(25)–N(23)–C(24)	110.8 (15)
C(13)–N(13)–Ni(1)	117.3 (13)	C(33)–N(23)–Ni(2)	113.3 (11)
C(13)–N(13)–C(4)	110.4 (13)	C(33)–N(23)–C(24)	112.4 (13)
C(13)–N(13)–C(5)	108.5 (15)	C(33)–N(23)–C(25)	107.0 (15)
C(9)–N(14)–Ni(1)	116.5 (10)	C(29)–N(24)–Ni(2)	117.6 (10)
C(12)–N(15)–Ni(1)	116.8 (9)	C(32)–N(25)–Ni(2)	116.4 (9)
C(15)–N(16)–Ni(1)	118.9 (12)	C(35)–N(26)–Ni(2)	118.3 (11)
C(2)–C(1)–N(11)	111.0 (12)	C(22)–C(21)–N(21)	109.3 (14)
C(1)–C(2)–N(12)	111.0 (13)	C(21)–C(22)–N(22)	113.2 (13)
C(4)–C(3)–N(12)	111.2 (14)	C(24)–C(23)–N(22)	108.5 (14)
C(3)–C(4)–N(3)	112.6 (17)	C(23)–C(24)–N(23)	113.0 (17)
C(6)–C(5)–N(13)	112.4 (15)	C(26)–C(25)–N(23)	114.2 (18)
C(5)–C(6)–N(11)	113.6 (15)	C(25)–C(26)–N(21)	109.5 (16)
C(8)–C(7)–N(11)	112.1 (12)	C(28)–C(27)–N(21)	115.8 (13)
C(9)–C(8)–C(7)	113.0 (15)	C(29)–C(28)–C(27)	115.0 (15)
C(8)–C(9)–N(14)	110.1 (16)	C(28)–C(29)–N(24)	111.1 (13)
C(11)–C(10)–N(12)	115.0 (13)	C(31)–C(30)–N(22)	115.1 (13)
C(12)–C(11)–C(10)	113.3 (13)	C(32)–C(31)–C(30)	114.5 (15)
C(11)–C(12)–N(15)	110.0 (15)	C(31)–C(32)–N(25)	112.8 (15)
C(14)–C(13)–N(13)	116.3 (17)	C(34)–C(33)–N(23)	113.3 (19)
C(15)–C(14)–C(13)	115.0 (14)	C(35)–C(34)–C(33)	114.3 (14)
C(14)–C(15)–N(16)	112.3 (16)	C(34)–C(35)–N(26)	108.7 (15)

[a] Estimated standard deviations are given in parentheses.

are approximately 93° when N(1) and N(2) are both involved and approximately 87° when two nitrogens of the tacn ring are considered. The coordination is thus elongated along the 3-fold axis. The trans N atoms and the Co atom are near linearity (179.2°). The rest of the angles might be expected to be close to the tetrahedral value, but this is not so. The nitrogen angles in the six-membered ring have much higher values, 117.0 (5)° at N(1) and 121.3 (5)° at N(2) (primary amine). The angles subtended by the carbon atoms of the propyl group are also larger than the tetrahedral value (113.1 (7)°). The distortion observed in the propyl side arms is comparable to that observed in Co[III]-(pn)$_3$[28] (pn = 1,3-diaminopropane), where the angles at the nitrogens are 122° (mean), the angles at the carbon atoms are 113.6° (mean), and the chelate bite angles are 91° (mean). Thus, the structure of compound A appears to be a simple composite of the structures of Co[III](pn)$_3$ and half of Co(tacn)$_2$. Any strain produced in bringing the two structures together is relieved by the slight elongation of the Co–N bonds.

In Table V are presented the interatomic distances for the nickel complex, compound B. This table is arranged so that each column contains the data for one molecule. The atomic labeling scheme of molecule 1 is visible in Figure 2. Molecule 2 is labeled in a similar way (add 10 and 20 to the N and C atom numbers, respectively). The mean Ni–N bond length is 2.14 Å, which again is longer than the normal Ni–N bond length (2.12 Å) expected for high-spin Ni(II)[26] but comparable to the Ni–N bond lengths (2.13 and 2.16 Å) observed in Ni[II](pn)$_3$.[29] The rest of the bond lengths fall in the normal range expected. The bond angles for compound B are given in Table VI, with each molecule having a separate column. There is a great similarity between the two molecules. The Ni atoms subtend small angles to the macrocyclic N atoms, of mean value 83.3° (of six), and a mean angle of 88.8° (of six) between the primary amine N atoms. The mean angle between trans ligands is 175.5° (of six). The angles N(primary)–Ni–N(tertiary) are divided by the molecular twist discussed later into two sets of six, a chelating set (mean 92.4°) and a nonchelating set (mean 95.5°). The angles at nitrogen are interesting because they show larger values in the six-membered rings, mean 116.6 (of six), which are comparable to those in the

(28) Nagao, R.; Maromo, F.; Saito, Y. *Acta Crystallogr., Sect. B: Struct. Crystallogr. Cryst. Chem.* **1973**, *B29*, 2438.
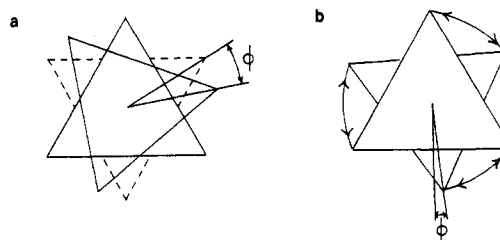(29) Andreetti, G. D.; Cavalca, L.; Sgarabotto, P. *Gazz. Chim. Ital.* **1971**, *101*, 494.

Figure 3. (a) Definition of twist angle. (b) Twist direction for compounds A and B.

cobalt compound, where the metal radius is smaller. The angles at the central C atoms of the propyl groups have a mean value of 113.2° (of six). The angles at the other C atoms of the six-membered rings have a mean value of 112.7° (of 12).

The angle of twist in the trigonal (or approximately trigonal) pendant arm structures under consideration is defined as the angular deviation (or the mean angular deviation for B) from the position most nearly related to octahedral coordination (see Figure 3a). Compound A has a small twist angle of 0.45°. Compound B has two independent cations with twist angles of 3.06 and 2.64°.

The cause of these angular distortions is the subject of considerable current discussion,[30] and the relationships between structure and reactivity that may be deduced from these relatively simple complexes have interesting implications.

Figures 1 and 2 are both drawn with the triazacyclononane part of the molecule in front. The five-membered chelate rings are in the $\delta\delta\delta$ or $\lambda\lambda\lambda$ configuration, depending upon the enantiomorphic choice, with which we are not concerned. The six-membered chelate rings are all in the chair configuration. In Figure 1 the propyl group is folded about the C(1)–C(3) line toward C(5), which is twisted (about the line from Co to the midpoint of the C(5)–C(4') bond) away from C(2). All three cations have this feature. In compound A (Figure 1) the C(2)···C(5) distance is 3.097 Å, which is close enough for a weak repulsion, but we would expect the interaction through bond torsion effects to be equally important. Thus, in Figure 1 linking N(1) to N(2) with the propyl group requires that C(1) be twisted toward N(2) about Co–N(1). Saturated five-membered rings of the ethylenediamine type are inherently nonplanar, and this effect in addition helps to pucker the triazacyclononane part of the ion into the conformation observed ($\delta\delta\delta$ or $\lambda\lambda\lambda$).

The component factors that determine structure cannot be readily separated. These are as follows: (1) the inherent nonplanarity of an isolated ethylenediamine ring, (2) cooperativity between the three rings, and (3) the additional effects of the three propylamine arms and the metal atom, including 6-ring to 6-ring and 6-ring to 5-ring interactions, having through-bond and through-space contributions.

It is the effect of the radius of the metal atom on which our data have particular bearing. The results show that the triazacyclononane ring differs in size between compounds A and B. The ethylenediamine type bites are 2.769 (10) and 2.85 (2) Å (mean), respectively. The bond lengths M–N are 2.025 (7) and 2.143 Å (mean). The angles formed at M are 86.3 (3) and 83.3° (mean) for A and B. The Ni complex is the more distorted from octahedral symmetry. Introducing the propylamine groups gives larger bite distances, 2.913 (10) and 3.129 Å (mean), respectively, for A and B. The increases relative to the ethylenediamine type bites are 0.144 and 0.279 Å, showing that the extension for the Ni complex is twice that of its Co analogue. This is indicative of a stress that is not fully resolved in compound B (the chelating bite in Ni^{II}(pn)$_3$[29] is only 2.96 Å). The trans angles are 179.2 (3) and 175.5° (mean), respectively. The primary amine part of the chelate encloses the Co atom well since the N(2)···N(2') distance (unlinked except through 12-membered ligand chains) is 2.749 Å, which is less than the ethylenediamine type bite for this complex. This is in keeping with the inertness[31] of this Co(III) complex toward capping reactions analogous to those carried out on Co^{III}(taetacn).[32] Sargeson[33] has also been unsuccessful in capping Co(III) complexes containing the tris(1,3-diaminopropane) moiety.

The structure of the Ni compound in contrast shows that the ligand is not holding the metal in such an unstrained way. The mean distance between the primary amine nitrogen atoms is 2.99 Å, that is, 0.14 Å greater than the ethylenediamine type bite in the same complex. The strain is seen both as the inability of the triazacyclononane moiety to expand enough and as less complete closure of the coordination at the primary amine positions relative to that in compound A. This is keeping with the lower stability and greater lability of compound B in chemical terms. The difference in the angles made by the trans ligands at M is also explained. The difference in M–N distance of 0.133 Å that we observe creates a need for ligand extension of 0.133π or 0.42 Å between antipodes on a great circle by simple geometry.

The tension in the ligand of the Ni(II) complex is the primary cause of the twist angle observed, 2.85° (mean). A larger number of torsion angles have been averaged to obtain the twist angles

Table VII. Electronic Spectral Data for Transition-Metal Complexes Derived from 1,4,7-Triazacyclononane

complex	λ_{max}, nm (ϵ, M^{-1} cm^{-1})	ref
Ni(taptacn)(NO$_3$)$_2$	340 (10), 538 (7.9), 815 (sh, 7.7), 860 (7.8)	this work
Ni(tacn)$^{2+}$	308 (12), 505 (7), 800 (7), 870 (sh)	4
Ni(dtne)$_2$$^{2+}$	363 (16), 516 (18), 848 (31), 917 (31)	34
Ni(taptacnH$_3$)$^{5+}$	363 (8.1), 598 (5.6), 785 (3.6), 910 (10)	this work[a]
Ni(taptacn)(ClO$_4$)$_2$	341 (8.9), 532 (7.2), 815 (sh, 14.5), 875 (15.5)	this work[b]
Ni(taptacn)$^{3+}$	358 (2.7 × 10^3), 625 (33)	this work
Co(taptacn)Br$_3$	358 (92.5), 497 (77.4)	this work
Co(tacn)$_2$$^{3+}$	333 (89), 458 (100)	4
Co(dtne)$^{3+}$	346 (230), 495 (323)	34
Co(taetacn)$^{3+}$	347 (198), 480 (242)	32
Co(taptacn)$^{2+}$	482 (12.7), 541 (sh, 4.4), 985 (10.3)	this work

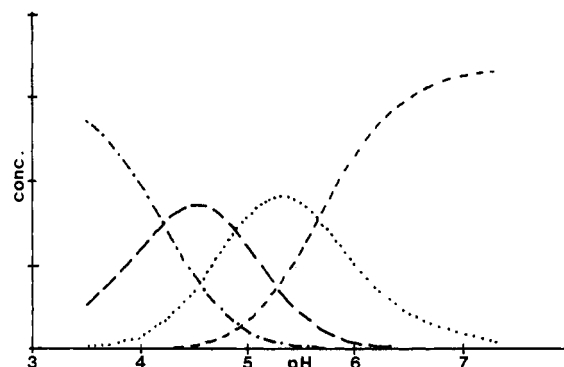[a] Measured in 1.0 M HClO$_4$. [b] Measured in CH$_3$CN.

Figure 4. Speciation curves for Ni^{II}(taptacn) as a function of pH: (- - -) Ni(taptacn)$^{2+}$; (···) Ni(LH)$^{3+}$; (- -) Ni(LH$_2$)$^{4+}$; (-·-) Ni(LH$_3$)$^{5+}$.

for compound B, and the details of these calculations have been deposited as supplementary material. The direction of the observed twists in compounds A and B is such as to close the torsion angles between propyl-linked nitrogen atoms of the type N(1)–Ce(1)–Ce(2)–N(2), where Ce denotes the centroid of an equilateral triangle (approximately in B). This direction is consistent with the idea of tension in, and extension of, the complete ligand framework of compound B relative to that of A.

Solution Studies. Electronic spectra are presented in Table VII. The nickel(II) species is purple, consistent with an NiN$_6$ chromophore in solution. The molar absorption coefficients, ϵ (M^{-1} cm^{-1}), of the d–d transitions are similar to those derived previously for species of this type (Ni(tacn)$_2$$^{2+}$,[4] Ni(dtne)$^{2+}$[34] (dtne = 1,2-bis(1,4,7-triaza-1-cyclononyl)ethane; see table VII).

In the case of the cobalt(III) species, the extinction coefficients for the first transition ($^1A_1 \rightarrow {}^1T_1$) are similar to those for other MN$_6$$^{3+}$ ions. However, for species based on the ligand dtne, the values are significantly greater. This has been attributed[34] to a trigonal twist enforced on the two triazacyclononane moieties. Similarly, Co^{III}(taetacn) also has unusually high extinction coefficients, and the trigonal twist calculated from its structural parameters[25] is 11.1°. In the present system, any effect of this nature is rendered much smaller owing to the presence of the propylene chain, which permits somewhat greater freedom of movement. This relaxation from a strained configuration is confirmed in the solid-state structure, where the trigonal twist for the cobalt(III) complex is 0.45°.

The fact that in the case of nickel(II) similar spectra are derived in both CH$_3$CN and CH$_3$NO$_2$ confirms that the inner coordination sphere remains intact in solution. However, in the presence of

(30) Comba, P.; Sargeson, A. M.; Engelhardt, L. M.; Harrowfield, J. M.; Horn, E.; Snow, M. R. *Inorg. Chem.* **1985**, *24*, 2325.

(31) Fortier, D. G.; McAuley, A., unpublished observations.

(32) Hammershoi, A.; Sargeson, A. M. *Inorg. Chem.* **1983**, *22*, 3554.

(33) Sargeson, A. M. *Pure Appl. Chem.* **1986**, *58*, 1511.

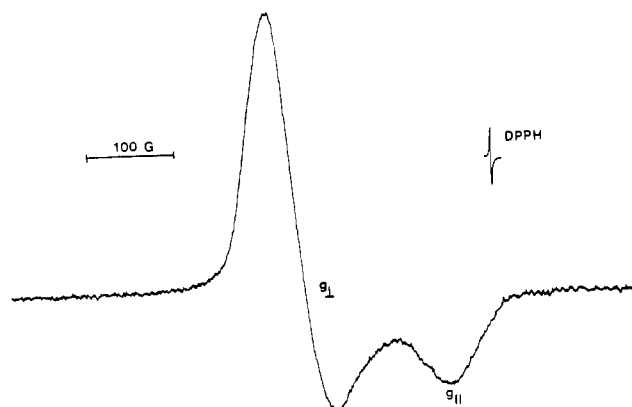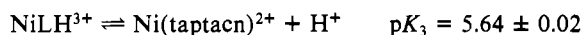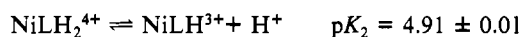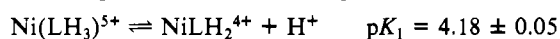(34) Wieghardt, K.; Tolksdorf, I.; Herrmann, W. *Inorg. Chem.* **1985**, *24*, 1230.

Figure 5. ESR spectrum of Ni^{III}(taptacn) in frozen CH_3CN.

acid (1.0 M $HClO_4$) ready dissociation of the coordinated primary amines takes place, with a significant change in the UV–visible spectrum. Three moles of H^+ is required for complete reaction, leading to a species where the three tertiary amines of the triazacyclononane remain coordinated with three water molecules occupying the other sites. Titrations carried out in both nitrate and chloride media (no detectable difference in results) over the pH range 3–11 were consistent with the fully coordinated taptacn ligand at pH ~ 7. Data are presented in Figure 4, and equilibrium data involving the mono-, di- and triprotonated species

$$Ni(LH_3)^{5+} \rightleftharpoons NiLH_2^{4+} + H^+ \quad pK_1 = 4.18 \pm 0.05$$

$$NiLH_2^{4+} \rightleftharpoons NiLH^{3+} + H^+ \quad pK_2 = 4.91 \pm 0.01$$

$$NiLH^{3+} \rightleftharpoons Ni(taptacn)^{2+} + H^+ \quad pK_3 = 5.64 \pm 0.02$$

show only a slight variation in the individual pK values, which are in the normal range for primary amines coordinated to a divalent metal center. On addition of base to a solution of Ni-$(LH_3)^{5+}$, $Ni(taptacn)^{2+}$ is formed immediately. Further protonation of the $Ni(LH_3)^{5+}$ species only occurs upon heating in 6 M HCl, generating LH_6^{6+} and $Ni(H_2O)_6^{2+}$. Owing to the instability of the Ni(III) complex, no similar experiments could be undertaken to compare the effect of increasing oxidation state. Protonation of the Co^{III}taptacn complex was not observed, as attested by the isolation of this complex from a cation-exchange column with 4 M HCl.

Oxidation of the nickel(II) complex may be achieved both chemically (Co^{3+} in neutral aqueous media or NO^+ in CH_3NO_2) and electrochemically (CV in CH_3CN shows a reversible wave, $E_{1/2} = 1.17$ V vs SCE). In the reaction with NO^+ ($E_{1/2} = 0.77$ V vs SCE in CH_3CN^{35}), an excess of oxidant is required to overcome the higher oxidation potential of the Ni complex. In aqueous media, oxidation is only observed at neutral pH, where the complex is fully coordinated. In acidic media, where the species $Ni(LH_3)^{5+}$ predominates, no oxidation occurs. Upon oxidation, in both aqueous and nonaqueous media, a lime green complex is produced (in aqueous medium, $\lambda_{max} = 358$ nm ($\epsilon = 2.7 \times 10^3$); λ_{max} is obscured by the excess NO^+ in the nonaqueous oxidation), which gives rise to an ESR spectrum with both $g_\parallel$ ($=2.033$) and $g_\perp$ ($=2.144$) features (Figure 5). This is characteristic of a low-spin Ni(III) d^7 system.

The nickel(III) complex is unstable in aqueous media, readily oxidizing water as expected from the high redox potential. However, the products (O_2 or H_2O_2) were not identified owing to the very low concentrations used in the reactions. Kinetic studies of the decomposition obeyed first-order laws, and plots of ln ($A - A_\infty$) vs time were linear for 5–6 half lives, giving a rate of (1.07 ± 0.05) $\times 10^{-2}$ s^{-1} ($t_{1/2} = 65 \pm 3$ s). Addition of acid immediately after the formation of the Ni(III) complex permits the study of the decomposition rate. It is observed (Table VIII) that the rate increases linearly with 1/[H^+] from 0.1 to 1.0 M $HClO_4$. This increase in decomposition rate indicates that the rate-determining

Table VIII. Rate Data for the Decomposition of Ni^{III}(taptacn)$^{3+}$ in Aqueous Media[a]

10^3[Ni^{III}]$_{in}$, M	[H^+], M	$10^2 k_{obsd}$, s^{-1}	10^3[Ni^{III}]$_{in}$, M	[H^+], M	$10^3 k_{obsd}$, s^{-1}
0.65	0.02	1.05	2.8	0.10	7.44
1.4		1.06		0.25	5.85
2.8		1.02		0.50	6.61
5.0		1.13		0.75	4.95
		1.07 $\pm$ 0.05 (av)		1.00	4.95

[a] Conditions: $T = 22$ °C, $I = 1.0$ M (ClO_4^-), $\lambda = 358$ nm.

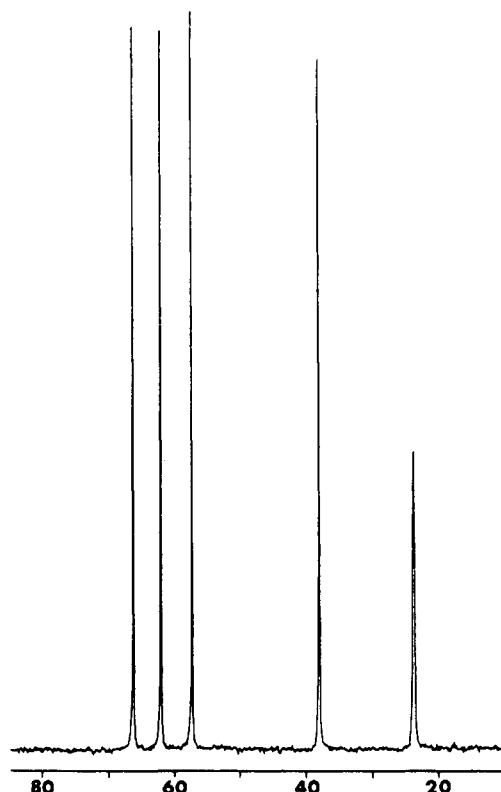**Figure 6.** ^{13}C NMR spectrum of Co^{III}(taptacn).

step in the decomposition is the outer-sphere oxidation of hydroxide ion by the fully coordinated nickel(III) complex. Any pathways involving dissociation of one or more of the pendant arms prior to oxidation of hydroxide would show an increase in rate with increasing [H^+], rather than a correlation with 1/[H^+]. One can thus conclude that the pK_a's of the Ni(III) complex are much lower than those of the Ni(II) species; this can be attributed to electrostatic factors linked to the greater charge on the metal center, and to somewhat stronger M–N bonds associated with the increase in oxidation state.

The cobalt(III) complex provides as expected an inert, diamagnetic d^6 ion. The ^{13}C NMR spectrum of this ion is shown in Figure 6 with five peaks as expected for a single isomer. The peak at 23.52 ppm is assigned to CCH_2C (C(2)) of the propyl arm and that at 37.95 ppm to the CH_2NH_2 carbon adjacent to the primary amine. The other features at 66.26, 62.08, and 57.33 ppm are associated with carbons adjacent to the tertiary nitrogens, CH_2N. The broadening of the C(2) peak can be attributed to coupling with the cobalt nucleus (^{59}Co, $I = ^7/_2$). The lack of a well-defined octet is due to quadrupolar broadening. Similar behavior has been observed for the ^{13}C NMR spectra of Sargeson's "sar" cage complexes[36] (sar = sarcophagine = 3,6,10,13,16,19-hexaazabicyclo[6.1.6]eicosane).

In 0.1 M $LiNO_3$ (pH ~ 6), the cyclic voltammogram shows a reversible wave (peak–peak separation 67 mV) with $E_{1/2} = -0.010$ V vs NHE. The value is intermediate between those of the strongly reducing $Co(tacn)_2^{3+/2+}$ ($E_{1/2} = -0.41$ V) and the

(35) Winfield, J., private communication.

(36) Lay, P. A.; Sargeson, A. M. *Inorg. Chem.* **1986**, *25*, 4801.

oxidizing Co(dpt)$_2$$^{3+/2+}$ ($E_{1/2}$ = +0.28 V; dpt = dipropylaminotriamine [N-(3-aminopropyl)-1,3-propanediamine]) complexes.[4] It has been suggested[34] that replacement of a secondary by a tertiary amine provides an electronic access to stabilization of the cobalt(II) ion. Also in the present system, the propylamine arms provide a means of accomodating more easily the reduced metal center of increased ionic radius. The crystal structure data confirm this aspect in that, as a result of the ligand geometry, Co–N bond lengths are 1.991 and 2.025 Å. The long Co^{III}–N bonds may be viewed as tending toward formation of a suitable ligand structure for the cobalt(+2) oxidation state in the +3 ion complex.

Wieghardt[4,37] has suggested a trend between the first d–d transitions ($^1A_1 \rightarrow {}^1T_1$) of CoN$_6$$^{3+}$ complexes and the redox potential of their Co(III/II) couples. An extensive survey of 32 cobalt(III) complexes shows some linearity, but the scatter is too great to identify a single line.[37] The data in the present study fall on this curve.

Kinetic Studies. Recent studies of the self-exchange rates of Co(III/II) complexes[31,38] have shown that encapsulation of the metal ion or the presence of a *bis*(triazacyclononane) framework greatly increases ($\sim 10^5$) the rate over that of the cobalt(III/II) hexaamine or tris(ethylenediamine) species. This has been ascribed to the fact[38] that, in the cobalt ammine complexes, the inner-sphere reorganization energies exceed those of the solvent spheres,[39] and structural factors may also be involved. (The reverse is true in the case of trithianonane complexes, where there are observed enhanced self-exchange rates.[38,40]) In the present system we have examined the self-exchange rate of the Co$^{III/II}$(taptacn) couple using both optically active forms of the reagents and by cross reactions with Co^{II}(sep)$^{2+}$ and Co^{II}(tacn)$_2$$^{2+}$.

As is seen from the ^{13}C NMR spectrum of Co^{III}(taptacn), only the fully coordinated species exists in solution (unlike the situation for the Ni(II) complex, where protonation of the pendant arms leads to partial dissociation). The Co(III) species exist as a pair of optically active enantiomers, which could not be completely separated by using a Sephadex C25 column (2 × 100 cm) and elution with sodium (+)-tartrate (0.2 M). However, sufficient enantiomeric excess (50%) was achieved in the initial and final fractions to enable kinetic studies to be undertaken. Reaction of (+)-Co^{III}(taptacn)$^{3+}$ (or (−)-Co^{III}(taptacn)$^{3+}$ with a racemic mixture of Co^{II}(taptacn)$^{2+}$ in deoxygenated aqueous solution was followed by using the method of Dwyer and Gyarfas,[41] by measurement of the change in optical rotation (r).[38,40] Under conditions of [Co(III)] ≈ [Co(II)], the rate law may be expressed in the form

$$-d[(+)\text{-Co}^{III}]/dt = k_{ex}[\text{Co}]_{total}$$

Plots of ln $[(r_t - r_\infty)/(r_0 - r_\infty)]$ vs t (where r_t is the optical rotation at any time t, r_0 is r at the beginning of the experiment, and r_∞ is r at equilibrium), were linear for 3–4 half-lives, and the self-exchange rate (see Table IX) was found to be 0.042 ± 0.005 M^{-1} s^{-1} (I = 0.1 M (LiNO$_3$); pH 9, 0.01 M sodium borate).

Outer-sphere reactions under similar conditions with Co(sep)$^{2+}$ ($E_{1/2}$ = −0.300 V, k_{11} = 5.1 M^{-1} s^{-1} [42]) and Co(tacn)$_2$$^{2+}$ ($E_{1/2}$ = −0.41 V,[4] k_{11} = 0.08 M^{-1} s^{-1} [38]) were also investigated (see Table IX). Self-exchange data may be derived by using the Marcus cross correlation[43,44]

$$k_{12} = (k_{11}k_{22}K_{12}f_{12})^{1/2}$$

$$\ln f_{12} = (\ln K_{12})^2/[4 \ln (k_{11}k_{22}/Z^2)]$$

(37) Ventur, D.; Wieghardt, K.; Nuber, B.; Weiss, J. *Z. Anorg. Allg. Chem.* **1987**, *551*, 33.
(38) Kuppers, H. J.; Neves, A.; Pomp, C.; Ventur, D.; Wieghardt, K.; Nuber, B.; Weiss, J. *Inorg. Chem.* **1986**, *25*, 2400.
(39) Endicott, J. F.; Kumar, K.; Ramasami, I.; Rotzinger, F. P. *Prog. Inorg. Chem.* **1983**, *30*, 141.
(40) Dubs, R. V.; Gahan, L. R.; Sargeson, A. M. *Inorg. Chem.* **1983**, *22*, 2523.
(41) Dwyer, F. P.; Gyarfas, E. C. *Nature (London)* **1950**, *166*, 481.
(42) Creaser, I. I.; Harrowfield, J. M.; Herlt, A. J.; Sargeson, A. M.; Springborg, J.; Geue, R. J.; Snow, M. R. *J. Am. Chem. Soc.* **1977**, *99*, 3182.

Table IX. Rate Data

(a) Rate Data for the Reaction of (+)-Co^{III}(taptacn)$^{3+}$ with Co^{II}(taptacn)$^{2+ a}$

10^3[Co^{III}], M	10^3[Co^{II}], M	[Co^{III}]/ [Co^{II}]	10^3[Co]$_{tot}$, M	10^4k_{obsd}, s^{-1}	10^2k_{exc}, M^{-1} s^{-1}
2.03	2.03	1.0	4.06	2.50	3.1
5.27	2.63	0.5	7.90	4.22	5.3
2.94	2.94	1.0	5.89	2.50	4.2
3.43	1.72	0.5	5.15	2.10	4.1
					4.2 ± 1.0 (av)

(b) Rate Data for the Reaction of Co^{III}(taptacn)$^{3+}$ with Co^{II}(sep)$^{2+ b}$

10^3[Co^{III}], M	k_{obsd}, s^{-1}	k_{12}, M^{-1} s^{-1}	10^3[Co^{III}], M	k_{obsd}, s^{-1}	k_{12}, M^{-1} s^{-1}
2.0	0.224		10.0	0.799	
	0.273			0.754	
	0.279			0.839	
	0.26 (av)	130		0.80 (av)	80
5.0	0.452				
	0.535				
	0.498				
	0.510				
	0.50 (av)	100			

$$k_{12}(\text{mean}) = 103 \pm 40 \text{ M}^{-1}\text{ s}^{-1}$$
$$k_{22}(\text{derived}) = 0.05 \pm 0.02 \text{ M}^{-1}\text{ s}^{-1}$$

(c) Rate Data for the Reaction of Co^{III}(taptacn)$^{3+}$ with Co^{II}(tacn)$_2$$^{2+ c}$

10^3[Co^{III}], M	k_{obsd}, s^{-1}	k_{12}, M^{-1} s^{-1}	10^3[Co^{III}], M	k_{obsd}, s^{-1}	k_{12}, M^{-1} s^{-1}
1.0	0.095		5.0	0.214	
	0.108			0.210	
	0.125			0.199	
	0.109 (av)	109		0.205 (av)	41
2.0	0.140		10.0	0.566	
	0.126			0.487	
	0.154			0.468	
	0.140 (av)	70		0.507 (av)	51

$$k_{12}(\text{mean}) = 68 \pm 30 \text{ M}^{-1}\text{ s}^{-1}$$
$$k_{22}(\text{derived}) = 0.03 \pm 0.02 \text{ M}^{-1}\text{ s}^{-1}$$

^{a}Conditions: T = 25.0 °C, I = 0.1 M (NO$_3$$^-$). ^{b}Conditions as for part a except [Co^{II}(sep)] = 1 × 10^{-4} M. ^{c}Conditions as for part a except [Co^{II}(tacn)$_2$$^{2+}$] = 1 × 10^{-4} M.

where k_{11} and k_{22} are the self-exchange rate constants for the individual self-exchange reactions, k_{12} is that for the cross reaction, and K_{12} is the overall equilibrium constant. Since the charges on all the reactants and products are the same and the ionic sizes roughly comparable, work terms were considered equal in all cases. With use of the relevant cross reactions, the self-exchange rate constant of the Co$^{III/II}$(taptacn) couple evaluated from the Co-(taptacn)/Co(sep) cross reaction is 0.05 ± 0.02 M^{-1} s^{-1} and from Co(taptacn)/Co(tacn)$_2$ is 0.03 ± 0.02 M^{-1} s^{-1}; these values are in excellent agreement with that obtained directly from the optical rotation data.

The rate constant is smaller (0.04 vs 0.08 M^{-1} s^{-1}) than that derived[38] for Co(tacn)$_2$$^{3+/2+}$. The value[31] for the Co(amsartacn)$^{3+/2+}$ couple (amsartacn = 9-amino-1,4,7,11,14,19-hexaazatricyclo[7.7.4.2^{4,14}]docosane), where one end of the cage is the tacn ring, is 0.086 M^{-1} s^{-1}. However, in the latter system two carbon atoms are present in the bridging arms.

The slower rate involving taptacn complexes when compared to the triazacyclononane system Co(tacn)$_2$$^{3+/2+}$ appears at first glance to be contrary to expectations. The longer Co^{III}–N bond lengths observed in Co^{III}(taptacn) might be interpreted to imply a smaller inner-sphere reorganization energy, assuming normal

(43) Marcus, R. A. *Annu. Rev. Phys. Chem.* **1964**, *15*, 155; *J. Phys. Chem.* **1963**, *67*, 853.
(44) Macartney, D. H.; Sutin, N. *Inorg. Chem.* **1983**, *22*, 3530.

Co^II–N bond lengths. But, the Co–N stretching frequency of Co^III(taptacn) is 519 cm^{-1} (identified by an 8-cm^{-1} shift upon deuteriation of the primary amines) compared to 479 cm^{-1} for Co^III(tacn)$_2$.[45] The greater force constant can then lead to a greater inner-sphere reorganization energy.

It has been shown recently that the self-exchange parameters of Co$^{3+/2+}$ couples may be treated in the framework of the Marcus–Sutin model for outer-sphere electron transfer.[38] For complexes of the type under consideration the preequilibrium constant (K_0) is 0.04 (I = 0.1 M) and radii (r) are 9.0 Å (with reaction thickness δ_r = 0.8 Å). From these values, a self-consistent set of parameters for the Marcus–Sutin model has been determined for the Co(taptacn)$^{3+/2+}$ couple: ΔG_{in}^{*} = 13.8 kcal/mol; ΔG_{out}^{*} = 5.2 kcal/mol, and $d_2 - d_3$ = 0.165 Å, yielding k_{exc} = 0.04 M^{-1} s^{-1} as observed in the present study. The somewhat smaller Δd value calculated for the present complexes is in keeping with the Co(III) species being slightly distorted toward the Co(II) structure

when compared to the structure of the Co(tacn)$_2^{3+}$ complex. However, a higher inner-sphere reorganization energy is postulated due to the increased force constants, thus rendering the self-exchange rate slower than for Co(tacn)$_2^{3+/2+}$.

(45) Boeyens, J. C. A.; Forbes, A. G. S.; Hancock, R. D.; Wieghardt, K. *Inorg. Chem.* **1985**, *24*, 2926.

Contribution from the Department of Chemistry, University of Victoria, Victoria, BC, V8W 2Y2 Canada

Crystal and Solution Structure of the Palladium(II) Bis(1,4,7-triazacyclononane) Ion: Evidence for Rapid Fluxional Behavior in a Macrocyclic Complex

G. Hunter,[†] A. McAuley,* and T. W. Whitcombe

An unusual example of fluxionality at the normally inert Pd(II) center is described. The preparation and X-ray crystal structure of the Pd(non)$_2^{2+}$ ion (non = 1,4,7-triazacyclononane) are presented. Pd(non)$_2$(PF$_6$)$_2$ crystallizes in the space group $P2_1/c$ with cell dimensions of a = 7.150 (1) Å, b = 16.675 (6) Å, c = 9.542 (3) Å, and β = 97.37 (2)° (Z = 2). In the solid state the ion displays square-planar geometry, Pd–N = 2.057 Å, with the third (noncoordinated) nitrogen atom in a configuration remote ($\sim$3.5 Å) from the metal center and the rings in an anti conformation. However, in solution at ambient temperatures, ^{13}C NMR shows only a single resonance, explicable only by a rapid ring hopping of the Pd(II) around the triaza macrocycle. This is considered to be the first example of such behavior for a Pd(II) amine complex. Temperature-dependence studies have permitted identification of syn and anti conformations in equilibrium ($K_{eq} \approx 2$). Rate data for the interconversion have been obtained, and a possible mechanism is proposed. The fluxional behavior of this ion explains the ready oxidation by air in aqueous medium to a very stable hexacoordinate Pd(III) ion.

Introduction

The importance of the use of small macrocycles such as 1,4,7-triazacyclononane (non) in the maintainance of geometrical configurations of metal complexes is being increasingly recognized. In the bis(ligand) metal complexes, octahedral geometry[1-5] is imposed as a result of the facial disposition of the donor atoms. However, dimeric species[6] of Fe(III) containing a μ-oxo bis(μ-acetato) core, a hemerythrin analogue,[7] and of Mn[8] may be formed where the facially coordinating tridentate ligand effectively caps the outer poles of the dimetal ion core. To date, most of the studies have been made on first-row elements, and much less information is available on second- and third-row congeners.[9-11] In addition to characterization, including X-ray data, a considerable interest has been shown in these species, since not only are they remarkably resistant to acid hydrolysis but also it is possible to prepare complexes in less common oxidation states. Generally, for the couples M(non)$_2^{3+/2+}$ (M = Ni,[3,4,12] Fe,[3,13,14] Co[2,15]) there is retention of configuration in the redox reactions. Rates of self-exchange and other redox parameters may be related[16,17] to the changes in the M–N inner coordination sphere distances upon electron transfer.

In this paper, we describe the preparation, crystal structure, and solution magnetic resonance features of the Pd(non)$_2^{2+}$ ion.

The structure is closely similar to that of the corresponding Pt(II) complex[9] Pt(non)$_2^{2+}$, where it is seen that only two of the three

(1) (a) Yang, R.; Zompa, L. J. *Inorg. Chem.* **1976**, *15*, 1499. (b) Zompa, L. J.; Margulis, T. N. *Inorg. Chim. Acta* **1978**, *28*, L157.
(2) Koyama, H.; Yoshino, T. *Bull. Chem. Soc. Jpn.* **1972**, *45*, 481.
(3) Wieghardt, K.; Schmidt, K.; Herrmann, W.; Kuppers, H. J. *Inorg. Chem.* **1983**, *22*, 2953.
(4) McAuley, A.; Norman, P. R.; Olubuyide, O. *Inorg. Chem.* **1984**, *23*, 1939.
(5) Kuppers, H. J.; Neves, A.; Pomp, C.; Ventur, D.; Wieghardt, K.; Nuber, B.; Weiss, J. *Inorg. Chem.* **1986**, *25*, 2400.
(6) Wieghardt, K.; Pohl, K.; Gebert, W. *Angew. Chem., Int. Ed. Engl.* **1983**, *22*, 722.
(7) Lippard, S. J. *Chem. Br.* **1986**, 222.
(8) Wieghardt, K.; Tolksdorf, I.; Herrmann, W. *Inorg. Chem.* **1985**, *24*, 1230.
(9) Wieghardt, K.; Koppen, M.; Swiridoff, W.; Weiss, J. *J. Chem. Soc., Dalton Trans.* **1983**, 1869.
(10) (a) Blake, A. J.; Holder, A. J.; Hyde, T. I.; Roberts, Y. V.; Lavery, A. I.; Schroder, M. *J. Organomet. Chem.* **1987**, *323*, 261. (b) Blake, A. J.; Gould, R. O.; Holder, A. J.; Hyde, T. I.; Lavery, A. J.; Odulate, M. O.; Schroder, M. *J. Chem. Soc., Chem. Commun.* **1987**, 118.
(11) Wieghardt, K.; Herrmann, W.; Koppen, M.; Jibril, I.; Huttner, G. *Z. Naturforsch., B: Anorg. Chem., Org. Chem.* **1984**, *39B*, 1335.
(12) Wieghardt, K.; Walz, W.; Nuber, B.; Weiss, J.; Ozarowski, A.; Stratemeier, H.; Reinen, D. *Inorg. Chem.* **1986**, *25*, 1650.
(13) Boeyens, J. C. A.; Forbes, A. G. S.; Hancock, R. D.; Wieghardt, K. *Inorg. Chem.* **1985**, *24*, 2926.
(14) Marsh, R. E. *Acta Crystallogr., Sect. B: Struct. Sci.* **1987**, *B43*, 174.
(15) McAuley, A.; Norman, P. R.; Olubuyide, O. *J. Chem. Soc., Dalton Trans.* **1984**, 1501.

[†] Present address: The University, Dundee, Scotland.